This paper is published as part of a *Dalton Transactions* themed issue on:

Bioinspired Catalysis

Guest Editor Seiji Ogo
Kyushu University, Japan

Published in issue 12, 2010 of *Dalton Transactions*

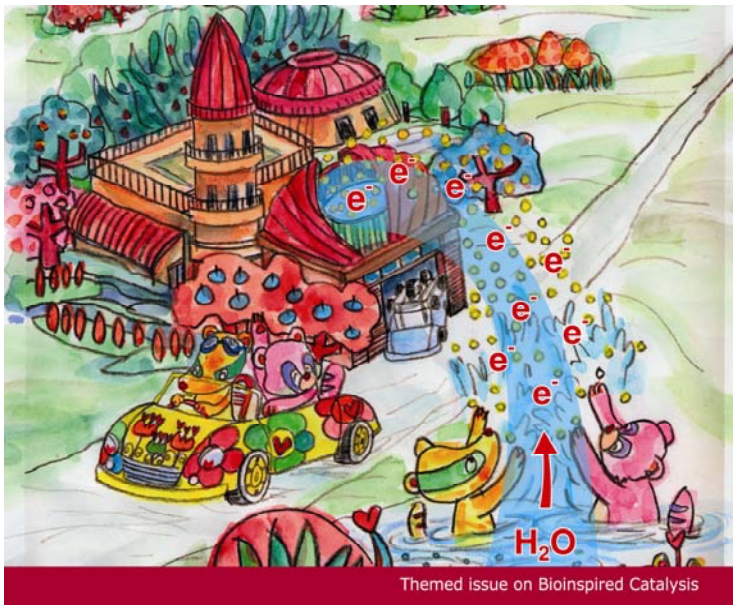

Image reproduced with permission of Seiji Ogo

Articles published in this issue include:

PERSPECTIVES:

Mimicking Nitrogenase
Ian Dance
Dalton Trans., 2010, DOI: 10.1039/b922606k

Dual functions of NifEN: insights into the evolution and mechanism of nitrogenase
Yilin Hu, Aaron W. Fay, Chi Chung Lee, Jared A. Wiig and Markus W. Ribbe
Dalton Trans., 2010, DOI: 10.1039/b922555b

Quest for metal/NH bifunctional biomimetic catalysis in a dinuclear platform
Takao Ikariya and Shigeki Kuwata
Dalton Trans., 2010, DOI: 10.1039/b927357c

COMMUNICATION:

Chemiluminescence enhancement and energy transfer by the aluminium(III) complex of an amphiphilic/bipolar and cell-penetrating corrole
Atif Mahammed and Zeev Gross
Dalton Trans., 2010, DOI: 10.1039/b916590h

Visit the *Dalton Transactions* website for more cutting-edge inorganic and bioinorganic research
www.rsc.org/dalton

Tuning the substrate specificity by engineering the active site of cytochrome P450cam: A rational approach

Soumen Kanti Manna and Shyamalava Mazumdar*

Received 2nd November 2009, Accepted 8th February 2010
First published as an Advance Article on the web 16th February 2010
DOI: 10.1039/b922885c

Rational design of the active site of cytochrome P450cam has been carried out to catalyse oxygenation of various potentially important chemical reactions. The modeling studies showed that the distal pocket of the heme consisting of the Y96, T101, F87 and L244 residues could be suitably mutated to change the substrate specificity of the enzyme. We found that the mutant enzymes could catalyse oxygenation of indole to produce indigo. While Y96F was found to be several times better as a catalyst for conversion of indole to indigo, the double mutant Y96F/L244A showed the highest NADH oxidation rate as well as yield of indigo. The oxidative catalysis using H_2O_2 as the oxygen source was found to produce a higher purity of indigo, and lesser or no formation of indirubin was detected. The enzymatic oxygenation of aromatic hydrocarbons such as coumarin and analogues was also found to be enhanced on mutation of Y96 and L244 residues in the enzyme. The studies also showed that mutation of suitable residues can alter the regio-selectivity of hydroxylation of the aromatic hydrocarbons.

Introduction

Functionalization of the C–H bond is at the heart of synthetic organic chemistry that leads to the production of the huge arsenal of organic molecules which are essential components of modern life.[1,2] The synthetic strategy to introduce a functional group generally involves the attachment of a heteroatom, often oxygen through oxidation, in place of the hydrogen atom of the C–H bond. In the traditional organic synthesis, the oxidation of the inert organic compounds are often requires high-valent heavy metal compounds like chromates, dichromates, chromyl chloride, ammonium cerium nitrate, bismuthate, vanadate, Ru-, Os-, Ir-, Pb-containing inorganic and organometallic compounds *etc.*[3,4] Many of these reagents show poor product selectivity and overall activity.[3] These heavy metal compounds and complexes are generally toxic and, therefore, biohazardous in nature.[5,6] For example, chromium(VI) compounds have been shown to be carcinogenic and mutagenic in nature.[7] In addition these reactions are almost invariably carried out in organic solvents and many commonly used organic solvents (*e.g.*, CH_2Cl_2, benzene, toluene, *etc.*) are suspected carcinogens and environmental pollutants (www.oehha.org/risk/ChemicalDB/index.asp and http://potency.berkeley.edu/index.html). Moreover, many of the oxidation reactions are carried out at extremes of pH, under higher pressure and at elevated temperature.[8] Thus it is essential to find out efficient but safe alternatives for carrying out organic synthesis in a more environmentally friendly manner.

Living organisms are outstanding examples of efficient reactors and all these reactions are carried out under ambient conditions by enzymes in water. Cytochrome P450s are the most versatile biological oxygenation catalysts. These enzymes can potentially oxidize almost any organic compound. The most common function of these enzymes is to carry out hydroxylation of organic compounds. However, they are also known to catalyze various other types of reactions such as epoxidation, dehydrogenation, dealkylation, dehalogenation *etc.*[9,10]

Apart from the fact that all of these reactions catalyzed by the enzyme take place under ambient conditions, they do away with any environmentally hazardous heavy metal or organic solvent. Thus the cytochrome P450s offer a potentially '***green***' alternative solution to the chemistry of oxidation of organic compounds.

Cytochrome P450cam (P450cam) has been one of the most exploited P450s for such a biotechnological application.[11] The native enzyme has long been shown to bind and catalyze the oxygenation of camphor analogues albeit with lower efficiency than that for camphor.[12] Lefever and Wacket reported the potential use of this enzyme for the degradation of the organochlorine compounds for the first time, where they showed that the wild-type enzyme can oxidize low molecular weight chloroalkanes.[13] The active site of the enzyme has been modified extensively by L.-L. Wong's group[14-21] at Oxford and others[22,23] to accommodate a variety of substrates, which are entirely different in size and structure compared to the natural substrate, 1*R*-camphor.

The P450cam variants have been shown to catalyze oxidation of both open chain as well as cyclic aliphatic compounds of different sizes such as, propane to heptane and substituted heptanes.[17] Several studies have demonstrated that they can catalyze the oxidation of different aromatic compounds, including polyaromatic hydrocarbons (PAH) as well.[15] The engineered P450cam variants have also been explored for fine chemicals synthesis.[16]

One of the most commonly used dyes by mankind since ancient times is indigo.[24] With the advent of organic chemistry, the industrial production of this dye has replaced the agricultural production by adopting the synthetic routes (see Fig. 1A & B) reported by Heumann in 1890 and later on by Pfleger in 1901.[25] In both cases, the synthesis not only involves harmful corrosive

Department of Chemical Sciences, Tata Institute of Fundamental Research, Homi Bhabha Road, Colaba, Mumbai, 400 005, India. E-mail: shyamal@tifr.res.in; Web: http://www.tifr.res.in/~shyamal; Fax: +91 22 2280 4610; Tel: +91 22 2278 2363

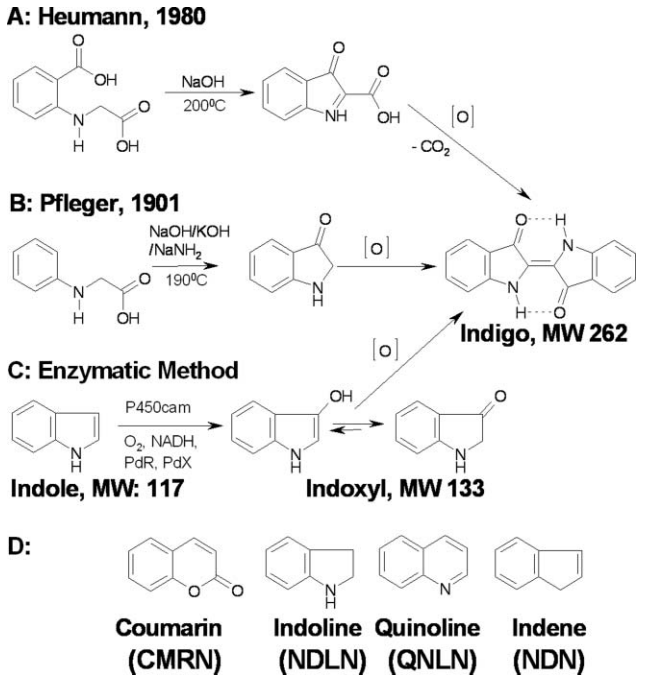

Fig. 1 Schematic representation of indigo synthesis through (A) Heumann's method, (B) Pfleger's method and (C) the proposed P450cam catalyzed pathway. (D) Shows the structures of hydrocarbons studied in the present report.

chemicals like NaOH or KOH at high temperatures but they are also carried out in organic solvents. In addition, *N*-phenyl glycine, the precursor for the industrial indigo production is synthesized from aniline using cyanide.[25]

The ancient as well as industrial production of this dye involves the synthesis of 3-hydroxyindole or indoxyl, which subsequently gets oxidized by aerial oxygen to indigo. The synthesis of indigo by heating in alkali solutions and the hydroxylated products of these reactions are often more toxic than the unsubstituted parent compounds.[25] We have explored the ability of the wild type and various specifically engineered P450cam variants to produce indigo from indole (Fig. 1C).

The hydroxylation of aromatic compounds involves nucleophilic attack of the hydroxyl group on the aromatic ring. The nucleophilic substitutions on aromatic rings are difficult and generally carried out under harsh conditions.[8] Moreover the tailor-made regio-selectivity of aromatic hydroxylation is difficult to achieve *via* conventional organic synthesis as the substitution takes place preferably at the *-ortho*/*-para* or *-meta* positions depending on the existing functional group on the aromatic ring.[8] However, in the case of the reactions by P450s the position of hydroxylation is dictated by the orientation of the substrate inside the active site. In view of the potential application of their hydroxyl derivatives,[26,27] we have selected a few important aromatic compounds (Fig. 1D) to test the feasibility of this hypothesis.

The reason for the high biological persistence of PAHs is the inability of the microorganisms to degrade them due to their chemical inertness and poor solubility. It has been shown that increases in the solubility increases the degradability of environmental pollutants.[28] Introduction of hydrophilic substituents like, the hydroxyl group, into these compounds is expected to increase the solubility and hence the bioavailability of these compounds for degradation. Moreover, biodegradation of many organic compounds (http://umbbd.msi.umn.edu/) has been shown to involve the oxygenation of the parent compound or the intermediate.[29] Thus the oxidation of the aromatic compounds by cytochrome P450cam could provide a ***'green'*** solution for a healthier environment.[15]

However, one of the main bottlenecks in the application of P450cam for biotechnological purposes remains the poor affinity of the enzyme for unnatural substrates. The catalytic cycle is turned on by the spin-state change at the heme active site due to expulsion of the axial water molecule on substrate binding, which is followed by electron transfer from NADH.[12] Poor substrate binding affinity and incomplete spin-transition has been shown to decrease the catalytic efficiency of the enzyme.[12] The present work mainly focuses on the enhancement of the binding affinity, high-spin content and electron transfer rate through rational redesign of the active site. The designs of the P450cam variants have been based on the following three point strategies:

1) Increase in the active site space for bigger molecules,

2) Decrease in the active site space for smaller and flatter molecules, and

3) The enhancement of the substrate binding affinity by complementary non-covalent interactions between the substrate and suitable amino acid side-chain in the active site.

We have taken the approach of site directed mutagenesis to achieve the goal, which if successful, would not only help to enhance the binding of the unnatural substrates but also provide useful information to understand the determinants of substrate–protein interactions that can be exploited for better design of the catalyst. Fig. 2 schematically represents the protein engineering strategy to accommodate unnatural substrates inside the P450cam active site. The binding affinity, electron transfer rate and the catalytic activity of the P450cam variants towards different substrates were measured to check the potential of these enzymes for biotechnological applications.

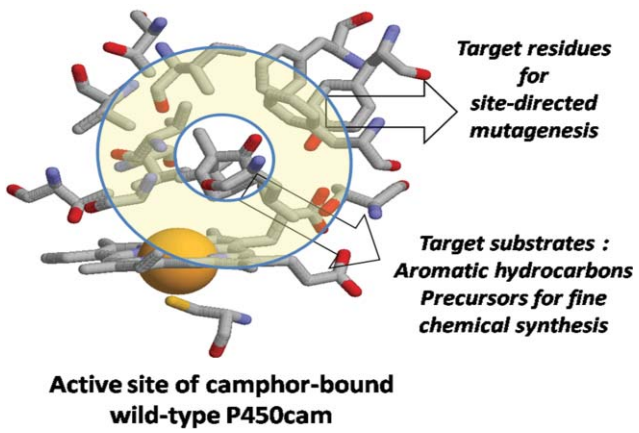

Fig. 2 Schematic representation of the active site engineering strategy to catalyze the oxidation of unnatural substrates using P450cam.

Experimental methods

Restriction enzymes and buffers for molecular biology works were obtained from New England Biolabs. DEAE-Sepharose,

Table 1 Primers used for preparing cytochrome P450cam mutants

Mutation	Restriction Site	Oligonucleotide primers
Y96F	Bsam I	5′ GCCGGCGAAGCaTtCGACTTCAT 3′
		5′ ATGAAGTCGaAtGCTTCGCCGGC 3′
Y96V	Bts I	5′GCCGGCGAAGCagtgGACTTCATTC 3′
		5′ GAATGAAGTCcactGCTTCGCCGGC 3′
Y96W	Hind III	5′ GCCGGCGAAGCtTggGACTTCAT 3′
		5′ ATGAAGTCccAaGCTTCGCCGGC 3′
F87W	Nco I	5′ GCGAGTGCCCaTggATCCCTCGTG 3′
	BamH I	5′ CACGAGGGATccAtGGGCACTCGC 3′
T101V	Cla I	5′ CTTCATTCCCgtaTCGATGGATCCG 3′
		5′ CGGATCCATCGAtacGGGAATGAAG 3′
Y96F/ T101V (FV)	Cla I	5′ CTTCATTCCCgtaTCGATGGATCCG 3′
		5′ CGGATCCATCGAtacGGGAATGAAG 3′
Y96F/ L244A (FA)	Sfo I	5′ GGATGTGTGGCgccTTACTGGTCGG 3′
		5′ CCGACCAGTAAggcGCCACACATCC 3‴

Q-sepharose and Sephadex G-25 columns were from Pharmacia Biotech. General Reagents, indole, coumarin, (1*R*)-camphor, 4-aminoantipyrene (4-AAP), hydrogen peroxide *etc.*, were from Sigma, India. UV-vis absorption spectra were measured on a Shimadzu (UV-2100) spectrophotometer coupled with a Peltier controlled thermostated cell holder. CD spectra were measured on a JASCO J-810 spectropolarimeter equipped with a Peltier cell temperature controller (±0.2 °C).

Mutation analysis

The $pCHC_1$ plasmid, encoding cytochrome P450cam C334A,[17] was a kind gift from Prof. L.-L. Wong (University of Oxford, UK). The plasmids encoding wild type putidaredoxin (PdX) and putidaredoxin Reductase (PdR) were kindly supplied by Prof. S. G. Sligar (University of Illinois, USA). The site directed mutagenesis of the cytochrome P450cam mutant were carried out using the Quikchange™ Site-Directed mutagenesis kit (Stratagene). The plasmids were isolated from freshly transformed *E. coli* (BL21DE3) cells and the purity was checked by running DNA gel (0.7% agarose). The primers for the P450cam mutants were designed in a way so that incorporation of the desired point mutations also introduces appropriate restriction sites into the P450cam gene (*camC*). The Table 1 shows the sequences of the primers used. The appearance of the characteristic bands compared to the wild type plasmid in the DNA gel of the digested plasmid was used to analyze and confirm the incorporation of the target mutation. The mutation of the enzyme was also confirmed by DNA sequencing as well as by comparing the agarose gels of the products of restriction digestion of the plasmid containing the mutation with those of the wild type enzyme.

Expression and purification of P450cam variants, putidaredoxin and putidaredoxin reductase

The cytochrome P450 variants were expressed following a slight modification of the reported method.[17] The first stage of purification of the wild type as well as the mutant P450cam involved passing of the crude cell lysate through a DEAE Sepharose ion exchange column using a salt gradient. This was subsequently desalted using a Sephadex G25 size exclusion column. The desalted protein was finally purified using a Resource-Q (6 ml, Amersham Biosciences) anion exchange chromatography column on an AKTA FPLC system (Amersham Biosciences). The purity of the protein was checked by both UV-visble spectroscopy ($A_{390}/A_{280} > 1.5$ or $A_{404}/A_{280} > 1.2$) and SDS-PAGE. The purified fractions were concentrated using an Amicon ultrafiltration membrane (YM-30, Amersham Biosciences) or Centricon tubes (3 kDa cut-off membrane, Amersham Biosciences) and stored with 40% (v/v) glycerol at −30 °C.

The wild type putidaredoxin (PdX) and putidaredoxin reductase (PdR) were purified using a reported procedure and the concentration of PdX was determined from the absorbance at 455 nm ($\varepsilon_{455} = 5.9\ mM^{-1}\ cm^{-1}$)[30] and that of PdR was estimated from the absorbance at 454 nm ($\varepsilon_{454} = 10.9\ mM^{-1}\ cm^{-1}$).[31]

NADH consumption rate

The NADH serves as the source of electrons during the catalytic cycle of the P450 enzyme to activate molecular oxygen and finally to hydroxylate camphor. The oxidation of NADH takes place by transfer of two electrons to P450cam through putidaredoxin reductase (PdR) and putidaredoxin (PdX). The reduced form of NADH shows an absorption band at 340 nm ($\varepsilon = 6.22\ mM^{-1}\ cm^{-1}$) which disappears on oxidation. The rate of NADH oxidation during catalysis was determined by monitoring the rate of change of absorption at 340 nm. The reaction mixture containing 1 μM PdR, 16 μM PdX, 0–1 μM P450cam variant, 100 mM KCl in 50 mM Tris (pH 7.4) was incubated at 25 °C to determine the background aerial oxidation rate in the absence of any catalysis. The catalytic reaction was initiated by addition of the substrate to the reaction mixture. The NADH oxidation rate was calculated from the slope of the initial linear part of the trace after subtraction of the background oxidation rate.

Indole oxidation

The oxidation of indole *via* the reductive cycle was performed in the presence of 0.2 μM PdR, 2 μM PdX, 0.2 μM P450cam variant, 100 mM KCl, 1 mM NADH and 0.5 mM indole in 50 mM Tris (pH = 7.4). The reaction mixture was kept at room temperature for two days and extracted with $CHCl_3$ for spectrophotometric or ESI-MS studies.

The oxidation of indole *via* the peroxide dependent oxidative cycle was performed in the presence of 4 μM P450cam variant, 100 mM KCl, 0–60 mM H_2O_2 and 0.5 mM indole in 50 mM Tris (pH = 7.4). The concentration of H_2O_2 ($\varepsilon_{200} = 200\ M^{-1}\ cm^{-1}$) stock was determined by spectrophotometry.[32] The indigo shows a characteristic absorption peak at 600 nm in $CHCl_3$. Thus the relative efficiency of indigo formation *via* indole oxidation by P450cam variants were expressed in terms of the absorbance of the $CHCl_3$ extract at 600 nm which represents the relative concentration of indigo. The control reactions for oxidative and reductive indole oxidation were carried out in the presence of all the ingredients in the respective catalytic mixtures except the P450cam variants. The purity of the indigo produced by the oxidative and reductive cycles was checked by thin layer chromatography (TLC) of the extracted product.

Oxidation of aromatic compounds

The formation of phenolic compounds on hydroxylation of the aromatic hydrocarbons by P450cam variants in the reductive cycle was checked by the 4-aminoantipyrene (4-AAP) assay for phenolic compounds.[33] The catalytic reaction mixture containing 0.2 μM PdR, 4 μM PdX, 0.4 μM P450cam variant, 100 mM KCl, 1.25 mM NADH and 0.5 mM coumarin in 50 mM Tris (pH = 7.4) was incubated at room temperature for 6 h. After the incubation, 2 μl 4-AAP (4% stock in DMSO) and 6 μl 10% ammonium persulfate (APS) were mixed with the reaction mixture along with 40 μl saturated $NaHCO_3$ solution and kept at room temperature for 30 min to complete the reaction.

Oxidation of the substrates by mutant P450cam

The catalytic reaction mixture containing 1 μM PdR, 10 μM PdX, 0.1 μM P450cam variant, 0.2 mM NADH, 100 mM KCl, and 0.1 mM substrate in 50 mM Tris (pH = 7.4) was extracted in $CHCl_3$ after completion of NADH oxidation. The reaction products were analysed by Electrospray ionization mass spectrometry (ESIMS) using a LCQ Deca (Thermo-Fisher) mass spectrometer. The chloroform extract was mixed with methanol (1 : 1) and injected into the ESI source of the instrument, at a flow rate of 5–10 μL min^{-1}, with 0.1% TFA to promote protonation of the organic molecules. The source voltage was kept at +4.5 kV for all experiments to create positively charged droplets which were finally detected and analyzed using a Quadrupole Ion-trap mass analyzer.

Results and discussion

Site specific mutation of P450cam

The substrate binding pocket of P450cam is lined with several residues which have been shown to be involved in substrate binding and catalysis by the enzyme.[12] We designed mutations of the F87, Y96, T101 and L244 residues to create a series of site-specific mutants of P450cam and assayed the efficiency of these mutants. The nature of the mutation was decided on the basis of the type of substrate to be catalysed. Thus larger and hydrophobic amino acids at the Y96 position were designed to accommodate flat aromatic molecules more efficiently than the wild type enzyme. Double mutations of the Y96F were also designed with T101V and L244A mutations for reactions of indole as well as of coumarin. The primers designed for mutations were such that each mutant produced a restriction site in the gene (Table 1), *e.g.*, the double mutant F96F/L244A was made using the pair of primers that introduces a new cleavage site for the restriction enzyme SfoI, while such a restriction site was absent in the DNA of the Y96F mutant. Agarose gel electrophoresis of the restriction digestion products of the mutant plasmid was compared with that of the wild type plasmid as shown in Fig. 3 and observation of the presence of the new restriction site in the plasmid confirmed the success of the mutation. The sequence of the mutant gene was also confirmed by DNA sequencing wherever required.

Each of the mutant enzymes was expressed and purified for further studies of substrate binding and enzymatic activity studies. The mutations designed in the present study were found to have no significant effect on the electronic environment around the heme active center of the enzyme and the UV-visible absorption spectra of the mutant P450cam enzymes were similar to that of the wild type enzyme with characteristic Soret absorption at 417 nm and visible bands at ~530 nm and ~570 nm in the absence of any substrate as shown in Fig. 4A. The overall structure of the mutant enzyme was also identical to that of the wild type species as indicated by the circular dichroism spectra of the enzymes in the far-UV region (Fig. 4B). Analyses of the far-UV CD showed the presence of ~40 ± 1% α-helical structure which agrees with the crystal structure of the wild type enzyme.[12] The tertiary structure around the heme was also not drastically altered on mutation and the visible CD spectrum of the mutants as shown in Fig. 4C is similar to that of the wild type enzyme although the relative ratios of the visible CD bands of the mutants were slightly different than that of the wild type enzyme owing to the small change in the substrate binding site of the enzyme.

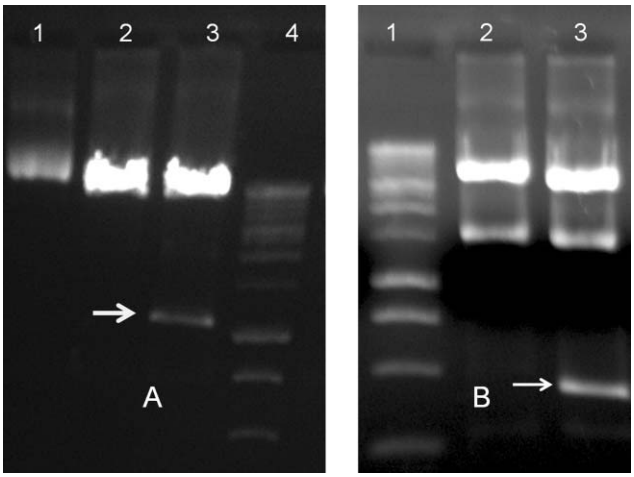

Fig. 3 Agarose gel electrophoresis of plasmid DNA and the restriction digestion of the mutant P450cam (A) Undigested Y96F plasmid (lane 1), Sfo I digested Y96F (lane 2) and Y96F/L244A (lane 3) plasmid along with BenchTop 1 kb DNA Ladder marker (lane 4). (B) BenchTop 1 kb DNA Ladder marker (lane 1) along with Bts I digested wild type (lane 2) and Y96V (lane 3) plasmid.

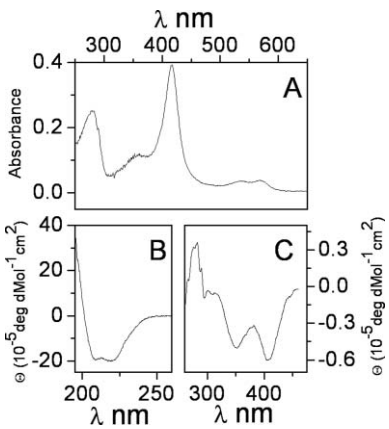

Fig. 4 Absorption spectra of the substrate-free (A) Y96F mutant of P450cam. (B) Far-UV CD spectra of substrate-free P450cam. (C) Near-UV and visible CD spectra of substrate-free Y96F mutant of P450cam.

Table 2 NADH oxidation rate of P450cam variants in the presence of indole (0.5 mM)

Variant	WT	Y96F	Y96F/L244A	Y96V
NADH oxidation rate (nmol/nmolP450/min)	4 ± 1	21 ± 3	24 ± 2	7 ± 2

The Y96 position has been shown to form hydrogen bonds with camphor in the substrate bound wild type enzyme.[12] The T101 residue was shown to be involved in stabilization as well as substrate binding in the wild type P450cam.[34] Extensive site specific mutations of Y96, F87, L244 and several other residues have been reported in the literature to alter the substrate specificity of P450cam.[12,14,15,19,21,23] L.-L Wong *et al.*, showed that combinations of mutations such as Y96F, F87A, F87L, F87W, and V247L could alter the substrate recognition as well as product selectivity of the enzyme for α-pinene, aromatic halides *etc.*[14,17,19,20] Enzymatic reactions of 2-ethylhexanol were reported using F87W, Y96W, T185F and L244A mutants of P450cam.[22] However, the enzymatic studies on mutation at the T101 site and combinations of T101V with Y96 mutations have not been reported earlier. The reactions of indole, coumarin and other aromatic hydrocarbons, that have been studied in the present report, uses some of these known mutants along with some new mutants of the enzyme.

Synthesis of indigo from indole using P450cam mutants

The addition of indole to the substrate-free P450cam variants was not found to cause any significant change in the absorption spectrum of the enzyme. However, the P450cam variants were found to oxidize NADH in presence of the substrate. These results indicate that although there is no change in the steady state spin equilibrium of the heme on binding of indole, it possibly produces transient high-spin species, which may get reduced by electrons from NADH and catalyze the oxygenation of indole. The results (Table 2) also showed that the NADH consumption rates for P450cam mutants like Y96F and Y96F/L244A (FA) were, respectively, ~5 and 6 fold higher than that of the wild type (WT) enzyme. Although the WT enzyme showed small NADH oxidation activity in the presence of the indole (Table 2), there was no detectable formation of indigo in the presence of the WT enzyme. On the other hand, the P450cam mutants (Y96F, Y96F/L244A and Y96V) were found to produce the blue dye (Fig. 5A) through the reductive cycle. The absorption spectra of the $CHCl_3$ extract of the catalytic mixture containing these mutant enzymes were found to consist of the characteristic peak of indigo at 600 nm (Fig. 5B). The ESI-MS spectrum (Fig. 6) of the extract showed peaks of unreacted indole along with that of indigo at m/z values of 147 (indole + H^+) and 263 (indigo + H^+). This also showed a small peak at $m/z = 134$ corresponding to indoxyl suggesting that the formation of indigo, indeed, proceeded *via* oxidation of indole at C_3 as proposed in Fig. 1C. The relative concentration of indigo was measured from the absorbance of the $CHCl_3$ extract at 600 nm. The results (Fig. 7) showed that the Y96F/L244A mutant is most efficient in conversion of indole to indigo, followed by Y96F and the Y96V mutants, through the reductive cycle.

Mutations of Y96 residue to Val and Phe increase the hydrophobicity of the substrate binding pocket in the Y96V and

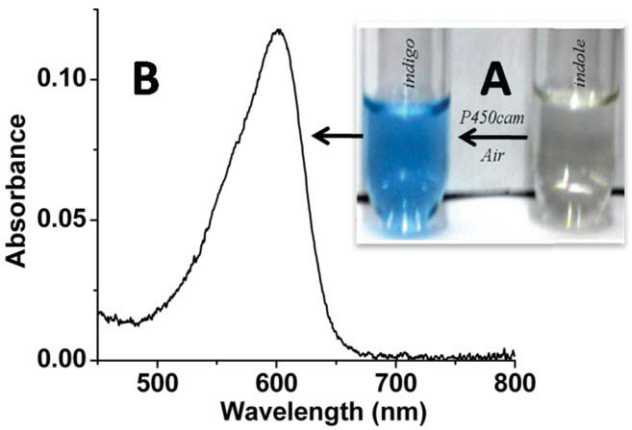

Fig. 5 (A) Indigo synthesis from indole oxidation by P450cam variants and (B) the absorption spectra of the indigo in $CHCl_3$.

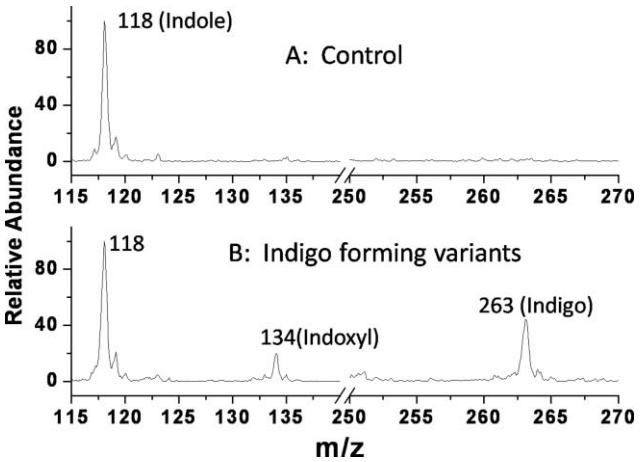

Fig. 6 ESI-MS spectrum of the $CHCl_3$ extract of the reaction mixture (A) in the absence of P450cam and (B) in the presence of Y96F. The numbers indicate the m/z value of the respective peaks.

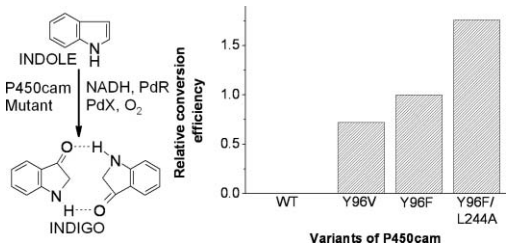

Fig. 7 Relative efficiency of indigo production by P450cam variants in the reductive cycle.

Y96F mutants. This possibly increases the residence time of the organic molecule in the pocket compared to the WT enzyme and thus increases the NADH oxidation rate and the probability of hydroxylation of indole. In the case of the Y96F/L244A mutation the efficiency of indole oxidation is further enhanced possibly due to creation of a larger space on the decrease of the chain length of the 244th residue, which is placed on top of heme. This might allow the planar indole molecule to access the distal site more easily facilitating the hydroxylation of indole by the putative oxo-ferryl species.[12] However, since the binding of indole cannot efficiently remove the water molecules from the active site,

uncoupling reactions may take place leading to poor efficiency of indole oxidation through the reductive cycle. Consequently, a significant amount of indole remains unreacted and the ESI-MS spectrum of the $CHCl_3$ extract of the reaction mixture, even after reaction for 2 days, shows an intense indole peak (Fig. 6).

One of the limiting factors in the application of P450cam is the requirement of the expensive cofactor (NADH) and the electron transfer partners (PdR and PdX). However, the peroxide shunt pathway[12] provides a more economic and easier method for the oxidation of organic compounds. Several P450cam mutants were found to carry out peroxide dependent oxidation of substrates.[35-37] We have studied whether the Y96F, Y96V and Y96F/L244A mutants could carry out the catalysis of indole oxidation through oxidative pathways using the 'Peroxide Shunt'.[12]

The indole was not found to be converted to indigo by H_2O_2 in the absence of the P450cam variants. The wild type enzyme as well as the Y96V mutant was also not found to cause any significant indigo production in the presence of H_2O_2. However, the Y96F and the Y96F/L244A mutants were found to significantly enhance the indigo formation from indole in the presence of H_2O_2. The results (Fig. 8A) showed that the increase in the H_2O_2 concentration increases the production of indigo for both of these mutants. However, the increase in the indigo production with H_2O_2 concentration was relatively more in presence of the Y96F/L244A (Fig. 8B) compared to that in presence of the Y96F mutant. Thus the Y96F/L244A mutant was found to have a higher efficiency of conversion of indole to indigo in the reductive as well as the oxidative cycle compared to the Y96F mutant.

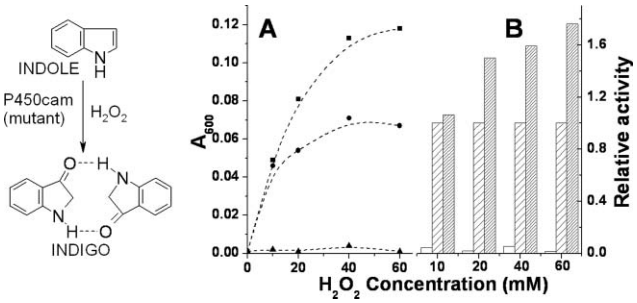

Fig. 8 (A) Variation of indole production with H_2O_2 concentration in the oxidative cycle in presence of Y96F/L244A (squares), Y96F (circles) and Y96V (triangles) mutants of P450cam. (B) Relative efficiency of indigo production at different H_2O_2 concentrations in the presence of Y96F/L244A (dense bars) and Y96V (empty bars) normalized with respect to that in presence of the Y96F (sparse bars) mutant of P450cam.

The product selectivity is a very important issue with respect to the viability of application of a synthetic scheme. Several studies have shown that the synthesis of the blue dye, indigo, is often associated with co-production of a isomeric pink dye, indirubin.[38] In fact, *in vivo* synthesis of indigo from indole using P450cam variants (with mutations at the 96th and 98th position), recombinant human CYP2E1 as well as toluene-4-monoxygenase have been reported to be associated with co-formation of indirubin.[39,40] Hence the purity of the *in vitro* indole oxidation products in the reductive as well as the oxidative cycle was checked using TLC.

The chromatogram (Fig. 9) showed that the indole oxidation product formed in the reductive cycle consisted of indirubin (pink band) along with indigo (blue band). However, the product of the oxidative cycle was found to consist of a single blue band corresponding to indigo. This suggests that the *in vitro* method of indigo synthesis *via* the oxidative cycle of P450cam is associated with a higher product selectivity compared to the reductive cycle or to the *in vivo* method.[40]

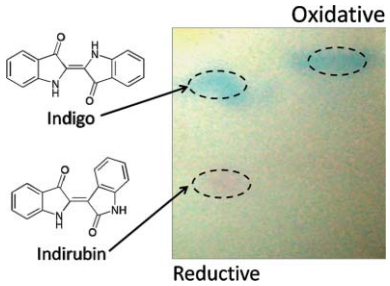

Fig. 9 Thin layer chromatogram of the indole oxidation product *via* the reductive and the oxidative cycle in the presence of the Y96F mutant.

Interaction of aromatic hydrocarbons with P450cam mutants

The addition of the aromatic compounds (Fig. 1D) was found to have no significant effect on the UV-visible absorption spectra of the WT P450cam. However, the absorption spectra of the mutants were found to undergo significant change on addition of these compounds. In contrast to that in case of indole, the addition of indoline (NDLN) to the P450cam variants was found to induce a red shift in the Soret maxima (Fig. 10A) and a Type II change in the difference spectrum (Fig. 10B). This indicates the formation of a direct Fe–N coordination in the enzyme–substrate complex. In the case of indole the lone pair of nitrogen resides in a conjugated 'p' orbital as a part of the Huckel (4n+2) aromatic 'π' electron system and therefore is not available for coordination to the iron center of the enzyme. But in the case of indoline the nitrogen lone pair resides in an 'sp^3' orbital. Thus indoline nitrogen can easily coordinate to the iron center leading to a Type-II shift in the difference spectra of the enzyme. Similarly, quinoline (QNLN) also forms a direct Fe–N coordination as indicated by a Type-II shift in the difference spectra. However, since the nitrogen lone pair in quinoline resides in an 'sp^2' orbital, it coordinates less strongly

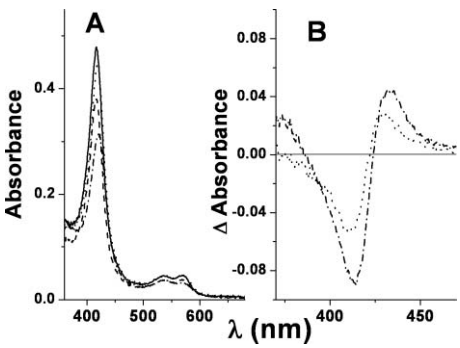

Fig. 10 The representative (A) absolute and (B) difference spectra of quinoline (dotted line) and indoline (dash-dotted line) binding to the substrate-free Y96F/L244A mutant (solid and dashed lines) of P450cam. The enzyme and final substrate concentrations for the quinoline and indoline binding were 4.5, 128 μM and 3.5, 63 μM, respectively.

Table 3 Spectroscopic binding constant (K_b in μM^{-1}) of aromatic hydrocarbons to P450cam variants

Substrate	WT	Y96F	FA[a]	FV[a]	Y96V	Y96W	F87W	T101V
CMRN	$(1.4 \pm 0.1) \times 10^{-3}$	$(7.3 \pm 0.2) \times 10^{-3}$	$(8 \pm 1) \times 10^{-3}$	$(8.1 \pm 0.5) \times 10^{-3}$	$(2.9 \pm 0.3) \times 10^{-3}$	$(1.3 \pm 0.4) \times 10^{-3}$	$(1.8 \pm 0.4) \times 10^{-3}$	$(11 \pm 1) \times 10^{-3}$
NDN	NA[a]	0.15 ± 0.01	0.19 ± 0.03	0.12 ± 0.02	0.04 ± 0.01	NA	0.09 ± 0.02	0.23 ± 0.03
QNLN	NA	0.12 ± 0.01	0.07 ± 0.01	0.16 ± 0.02	NA	0.1 ± 0.01	NA	NA
NDLN	0.04 ± 0.02	0.15 ± 0.03	0.16 ± 0.02	0.14 ± 0.02	0.07 ± 0.01	0.04 ± 0.02	0.02 ± 0.01	0.08 ± 0.01

[a] 'NA' indicates no appreciable binding; FA:Y96F/L244A; FV:Y96F/T101V mutants of P450cam.

to the iron center compared to indoline. This was reflected by the fact the Soret peak in the absorption spectra as well as the peak of the difference spectra of the enzyme was slightly more red-shifted in the presence of indoline compared to that in the presence of quinoline. On the other hand the addition of indene (NDN) and coumarin (CMRN) showed a blue shift in the Soret peak (Fig. 11A) and a Type-I difference spectra (Fig. 11B) indicating that these compounds do not form any direct coordination to the iron center. The spectroscopic binding constants (Table 3) of the P450cam variants were determined for these substrates. The results showed that almost all the P450cam mutants, especially, Y96F, Y96V, T101V, Y96F/L244A and Y96F/T101V, had higher affinities for the aromatic hydrocarbons compared to the wild type enzyme. Quinoline was found to have a lower binding affinity compared to indoline in most of the cases. On the other hand indene binding constants were considerably higher than those for coumarin in most of the mutants. This may be attributed to the fact that indene is a more hydrophobic molecule compared to coumarin and thereby prefers to reside in the hydrophobic environment of the active site of the P450cam mutants more than coumarin.

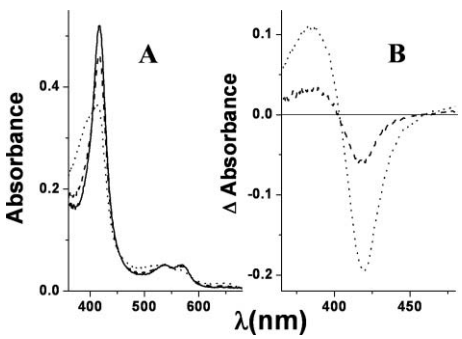

Fig. 11 The representative (A) absolute and (B) difference spectra of coumarin (dashed line) and indene (dotted line) binding to the substrate-free Y96F/L244A mutant (solid line) of P450cam. The final enzyme, indene and coumarin concentrations were 4.5 μM, 105 μM and 1 mM, respectively.

Table 4 gives the rate of NADH consumption for different P450cam mutants in the presence of various aromatic compounds. The results in Table 4 show that the NADH consumption rates in the presence of coumarin were significantly enhanced in the case of Y96F and Y96F/L244A (FA) mutants.

Coumarin was selected as a representative hydrocarbon substrate to evaluate the ability of the P450cam variants to oxygenate the aromatic hydrocarbons. The selection of coumarin was based on the facts that the hydroxycoumarin derivatives are used as drugs, dyes/sensors, sunscreen agents and also for the assay of microsomal P450s.[41-43] Thus selective hydroxylation of coumarin

Table 4 NADH consumption rates (nmol $nmol^{-1}$ P450/min) of P450cam variants in the presence of aromatic hydrocarbons (0.5 mM)

Substrate	WT	Y96F	FA[a]	FV[a]	Y96V	Y96W	F87W	T101V
CMRN	3 ± 1	30 ± 3	35 ± 3	3 ± 1	4 ± 1	2 ± 1	3 ± 1	2 ± 1
NDN	12 ± 1	194 ± 5	188 ± 7	29 ± 1	46 ± 4	7 ± 1	11 ± 1	14 ± 1
QNLN	2 ± 1	2 ± 1	5 ± 1	NA[a]	3 ± 1	2 ± 1	3 ± 1	3 ± 1
NDLN	14 ± 2	40 ± 2	33 ± 3	23 ± 3	26 ± 2	18 ± 2	22 ± 2	24 ± 1

[a] 'NA'indicates no appreciable reaction; FA:Y96F/L244A; FV:Y96F/T101V mutants of P450cam.

may find potential industrial application. The hydroxylation of this compound would increase the molecular weight by 16 mass units (Fig. 12). Thus the hydroxylated product is expected to show a peak at $m/z = 161$ ($162\text{-}H^+$) in the negative ion mode of the ESI-MS spectrum. The ESI-MS spectra of the $CHCl_3$ extract (Fig. 12) from the reaction mixture containing the WT enzyme did not show any significant peak intensity at $m/z = 161$ compared to the control. This indicated that the wild type enzyme does not have any measurable activity for hydroxylation of coumarin. However, most of the mutant enzymes catalyzed the hydroxylation of coumarin and distinct ESI-MS peak at $m/z = 161$ for hydroxyl coumarin was observed (Fig. 12C). Interestingly, though the NADH consumption rates (Table 4) for the Y96W, Y96V and Y96F/T101V mutants in the presence of coumarin were very small, these mutants, unlike the WT enzyme showed coumarin hydroxylation activity (Fig. 13).

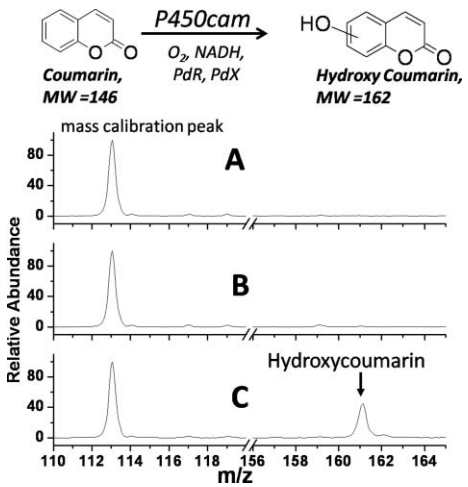

Fig. 12 The ESI-MS spectrum (negative ion mode) of the $CHCl_3$ extract of the catalytic mixture (A) in the absence of P450cam, (B) in the presence of the wild type enzyme and (C) in the presence of the Y96F/L244A mutant. The schematic representation of coumarin hydroxylation by P450cam variants is shown at the top panel.

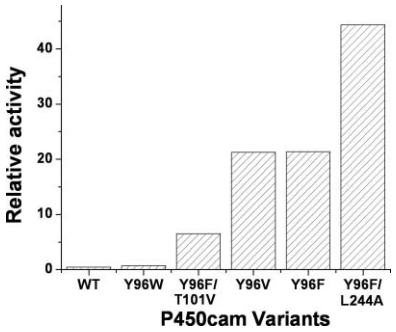

Fig. 13 Relative coumarin hydroxylation activity of P450cam variants in the reductive cycle with respect to the intensity of the ESI-MS peak at $m/z = 161$.

The results (Fig. 13) showed that the coumarin hydroxylation activity was enhanced respectively by ~ 2, 16, 52, 52 and 110 fold in the case of the Y96W, Y96F/T101V, Y96V, Y96F and Y96F/L244A mutant compared to the wild type enzyme. These mutants either reduce the mobility of the substrate by reducing the height of the substrate binding pocket (Y96W) or by increasing the hydrophobicity (Y96F/T101V, Y96F, Y96V) and the space on top of heme (Y96F/L244A) to help the planar substrate come closer to the putative oxo-ferryl species and, thereby, increase the substrate hydroxylation compared to the wild type enzyme. The present ESIMS results however, could not unambiguously identify the position of hydroxylation of coumarin in the enzymatic reaction (see below).

In order to determine the position of hydroxylation in coumarin, we carried out the assay of the enzymatic activity of the P450cam variants using 4-aminoantipyrene (4-AAP) for detection of hydroxycoumarins as described in the previous section. The reaction of 4-aminoantipyrene (4-AAP) in the presence of ammonium persulfate (APS) in mild alkaline solution with a phenolic compound produces a quinoneimine dye that could be detected spectroscopically. The 4-AAP assay of hydroxycoumarin, in the present case would give positive results when the *para*-position to the –OH group is vacant in the hydroxycoumarin to form the quinoneimine dye, that shows an absorption maximum at 467 nm (Fig. 14). The 4-AAP coupling reactions with coumarin in the absence of P450cam showed that the APS itself does not cause any significant aromatic hydroxylation under the conditions of the assay (control experiment). The wild type enzyme too did not show any appreciable hydroxylation of the aromatic ring of coumarin that could be detected by the 4-AAP assay. The quinoneimine dye, detected from the increase in absorbance at 467 nm (Fig. 14), formed by coupling of the 4-AAP at the -*para* position of the phenol was formed when mutants of P450cam were used for enzymatic hydroxylation of coumarin.

The results of the assay showed (Fig. 15) that the aromatic hydroxylation activity was enhanced by ~25, 100, 175 and 400 times in the presence of the Y96F/T101V, Y96F, Y96V and Y96F/L244A mutant, respectively, compared to that of the wild type enzyme. As the 4-AAP assay recognizes only those phenolic compounds, which have an open -*para* position for coupling (Fig. 14),[33] the present assay would measure the concentration of only 5- and 8-hydroxy coumarin products only. So the results suggest that the P450cam variants, especially, Y96F/L244A not

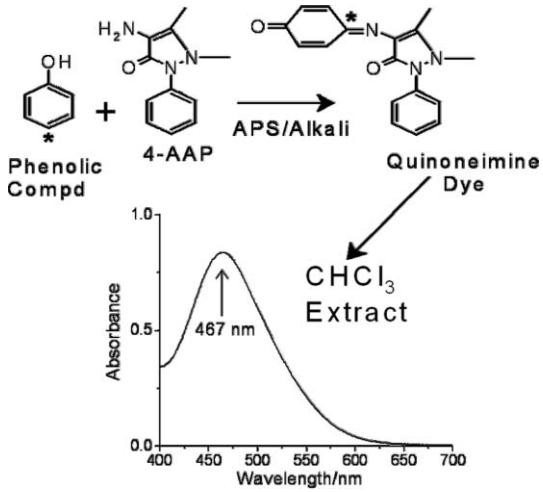

Fig. 14 Colorimetric assay for aromatic hydroxylation using 4-AAP coupling reaction. * represents the site of coupling reaction.

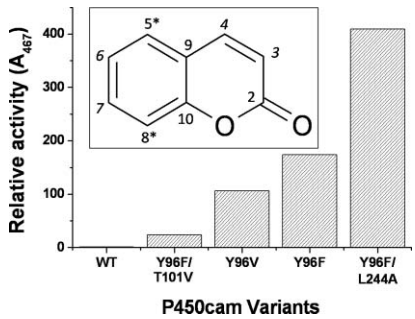

Fig. 15 Relative coumarin hydroxylation activity (at C5 and/or C8) of P450cam variants in the reductive cycle with respect to the wild type enzyme. (The inset shows the structure of coumarin with IUPAC numbering. The numbers followed by * show the hydroxylation sites sensitive to detection by 4-AAP assay and the numbers in italics represent other possible hydroxylation sites.)

only have a higher activity but also have a higher regio-selectivity for coumarin hydroxylation at C_5 and C_8 positions.

The results shown in Fig. 13 and Fig. 15 suggest that the relative yield of the coumarin hydroxylation product detected from the mass spectra were different from those by a 4-AAP assay of 5/8-hydroxycoumarin in the catalytic reactions of coumarin with different P450cam mutants. The ESI-MS detects a total yield of hydroxycoumarin while the 4-AAP assay would give a measure of only 5/8-hydroxycoumarin. The ratios of hydroxycoumarin produced by catalytic reaction of coumarin with Y96F/T101V, Y96V, Y96F and Y96F/L244A mutants of P450cam were 16 : 52 : 52 : 110 (~0.15 : 0.5 : 0.5 : 1). On the other hand the ratios of 5/8-hydroxycoumarin for the same reaction, under identical conditions, were 25 : 100 : 175 : 400 (~0.06 : 0.25 : 0.4 : 1) for the catalytic reactions in the presence of Y96F/T101V, Y96V, Y96F and Y96F/L244A mutants of P450cam.

Assuming that the Y96F/L244A mutant catalyzes regio-selective hydroxylation of coumarin to give solely 5- and/or 8-hydroxycoumarin the above results suggest that the ratios of total hydroxycoumarin to 5/8-hydroxycoumarin are 0.15 : 0.06, 0.5 : 0.25, 0.5 : 0.4 and 1 : 1, respectively for Y96F/T101V, Y96V, Y96F and Y96F/L244A mutants as catalysts.

Coumarin can undergo hydroxylation at C_3, C_4, C_6 and C_7 apart from at C_5 and C_8 positions (see inset of Fig. 15). The products of C_3, C_4, C_6 and C_7 hydroxylation would not give a positive 4-AAP test. The results indicate that the Y96F/T101V mutant of the enzyme possibly produces 1.5 times more hydroxylation at C_3, C_4, C_6 and C_7 positions compared to that at C_5 and C_8 of coumarin. Thus the above results show that the engineering of the active site of P450cam can be successfully exploited for the enhancement of activity as well as regio-selectivity of hydroxylation of aromatic compounds. However, it must be mentioned that the detailed and quantitative characterization of the enzymatic properties of the P450cam variants and the product distributions call for further studies.

Conclusions

Our study showed that the protein engineering of cytochrome P450cam can give a possible alternative route for the synthesis of the industrially important blue dye indigo. It also showed that the *in vitro* oxidative cycle is a cleaner method compared to the reductive cycle as well as *in vivo* synthesis of the dye from indole. The rational redesigning of the P450cam active site was found to enhance the affinity of the enzyme for unnatural substrates as well as the NADH oxidation rate in the presence of aromatic compounds. The engineering of the P450cam active site was found to enhance the activity of the enzyme for regio-selective hydroxylation of coumarin. The present studies thus demonstrate that the cytochrome P450cam can be successfully engineered for synthetic as well as environmental applications.

Acknowledgements

The Authors wish to thank Mr. Bharat T. Kansara for help. This work was supported by the Indo French Centre for the Promotion of Advanced Research (IFCPAR/CEFIPRA), New Delhi. The work was carried out at the Tata Institute of Fundamental Research, Mumbai.

References

1 E. J. Corey and X.-M. Cheng, *The Logic of Chemical Synthesis*, Wiley, New York, 1995.
2 K. Godula and D. Sames, *Science*, 2006, **312**, 67–72.
3 W.-M. Cheung, H.-Y. Ng, I. D. Williams and W.-H. Leung, *Inorg. Chem.*, 2008, **47**, 4383–4391.
4 J. M. Keith, R. J. Nielsen, J. Oxgaard and W. A. Goddard, 3rd, *J. Am. Chem. Soc.*, 2005, **127**, 13172–13179.
5 N. S. Loumbourdis, *Bull. Environ. Contam. Toxicol.*, 1997, **58**, 945–952.
6 J. O. Duruibe, M. O. C. Ogwuegbu and J. N. Egwurugwu, *Int. J. Phys. Sci.*, 2007, **2**, 112–118.
7 T. Norseth, *Environ. Health Perspect.*, 1981, **40**, 121–130.
8 F. A. Carey and R. J. Sundberg, *Part B: Reaction and Synthesis*, 4th edn, Kluwer Academic/Plenum Publishers, New York, 2001.
9 F. P. Guengerich, *Chem. Res. Toxicol.*, 2001, **14**, 611–650.
10 P. R. Oritz de Montellano and J. J. De Voss, in *Cytochrome P450: Structure, Mechanism, and Biochemistry*, ed. P. R. Oritz de Montellano, Plenum Press, New York, 3rd edn, 2005, pp. 183-246.
11 V. B. Urlacher, S. Lutz-Wahl and R. D. Schmid, *Appl. Microbiol. Biotechnol.*, 2004, **64**, 317–325.
12 E. J. Mueller, P. J. Loida and S. G. Sligar, in *Cytochrome P450: Structure, Mechanism, and Biochemistry*, ed. P. R. Oritz de Montellano, Plenum Press, New York, 2nd edn, 1995, pp. 83-124.
13 M. R. Lefever and L. P. Wackett, *Biochem. Biophys. Res. Commun.*, 1994, **201**, 373–378.
14 F. Xu, S. G. Bell, Z. Rao and L.-L. Wong, *Protein Eng., Des. Sel.*, 2007, **20**, 473–480.
15 C. F. Harford-Cross, A. B. Carmichael, F. K. Allan, P. A. England, D. A. Rouch and L. L. Wong, *Protein Eng., Des. Sel.*, 2000, **13**, 121–128.
16 R. J. Sowden, S. Yasmin, N. H. Rees, S. G. Bell and L. L. Wong, *Org. Biomol. Chem.*, 2005, **3**, 57–64.
17 J. A. Stevenson, A. C. Westlake, C. Whittock and L.-L. Wong, *J. Am. Chem. Soc.*, 1996, **118**, 12846–12847.
18 P. J. Jonathan, J. O. H. Ellen and W. Luet-Lok, *Eur. J. Biochem.*, 2001, **268**, 1460–1467.
19 S. G. Bell, X. Chen, F. Xu, Z. Rao and L. L. Wong, *Biochem. Soc. Trans.*, 2003, **31**, 558–562.
20 S. G. Bell, X. Chen, R. J. Sowden, F. Xu, J. N. Williams, L.-L. Wong and Z. Rao, *J. Am. Chem. Soc.*, 2003, **125**, 705–714.
21 D. P. Nickerson, C. F. Harford-Cross, S. R. Fulcher and L.-L. Wong, *FEBS Lett.*, 1997, **405**, 153–156.
22 K. J. French, D. A. Rock, J. I. Manchester, B. M. Goldstein and J. P. Jones, *Arch. Biochem. Biophys.*, 2002, **398**, 188–197.
23 V. Reipa, M. P. Mayhew, M. J. Holden and V. L. Vilker, *Chem. Commun.*, 2002, 318–319.
24 E. S. Ferreira, A. N. Hulme, H. McNab and A. Quye, *Chem. Soc. Rev.*, 2004, **33**, 329–336.
25 H. Zollinger, in *Color Chemistry: Syntheses, Propertiesand Applications of Organic Dyes and Pigments*, Wiley, 3rd edn, 2003, pp. 255-354.
26 R. Balamurugan, F. J. Dekker and H. Waldmann, *Mol. BioSyst.*, 2005, **1**, 36–45.
27 N. Au and A. E. Rettie, *Drug Metab. Rev.*, 2008, **40**, 355–375.
28 P. H. Lee, S. K. Ong, J. Golchin and G. L. Nelson, *Water Res.*, 2001, **35**, 3941–3949.
29 K. M. Weir, T. D. Sutherland, I. Horne, R. J. Russell and J. G. Oakeshott, *Appl. Environ. Microbiol.*, 2006, **72**, 3524–3530.
30 V. Y. Kuznetsov, E. Blair, P. J. Farmer, T. L. Poulos, A. Pifferitti and I. F. Sevrioukova, *J. Biol. Chem.*, 2005, **280**, 16135–16142.
31 I. F. Sevrioukova and T. L. Poulos, *J. Biol. Chem.*, 2002, **277**, 25831–25839.
32 R. A. Crowell, R. Lian, J. Sauer, M. C., D. A. Oulianov and I. A. Shkrob, *Chem. Phys. Lett.*, 2004, **383**, 481–485.
33 E. Emerson, *J. Org. Chem.*, 1943, **8**, 417–428.
34 S. K. Manna and S. Mazumdar, *Biochemistry*, 2006, **45**, 12715–12722.
35 B. Munge, C. Estavillo, J. B. Schenkman and J. F. Rusling, *ChemBioChem*, 2003, **4**, 82–89.
36 S. Jin, T. M. Makris, T. A. Bryson, S. G. Sligar and J. H. Dawson, *J. Am. Chem. Soc.*, 2003, **125**, 3406–3407.
37 H. Joo, A. Arisawa, Z. Lin and F. H. Arnold, *Chem. Biol.*, 1999, **6**, 699–706.
38 J. L. Royo, E. Moreno-Ruiz, A. Cebolla and E. Santero, *J. Biotechnol.*, 2005, **116**, 113–124.
39 A. Celik, R. E. Speight and N. J. Turner, *Chem. Commun.*, 2005, 3652–3654.
40 E. M. Gillam, A. M. Aguinaldo, L. M. Notley, D. Kim, R. G. Mundkowski, A. A. Volkov, F. H. Arnold, P. Soucek, J. J. DeVoss and F. P. Guengerich, *Biochem. Biophys. Res. Commun.*, 1999, **265**, 469–472.
41 A. Singh, K. Chen, S. J. Adelstein and A. I. Kassis, *Radiat. Res.*, 2007, **168**, 233–242.
42 K. Nakamura, I. H. Hanna, H. Cai, Y. Nishimura, K. M. Williams and F. P. Guengerich, *Anal. Biochem.*, 2001, **292**, 280–286.
43 B. Thati, A. Noble, B. S. Creaven, M. Walsh, M. McCann, K. Kavanagh, M. Devereux and D. A. Egan, *Cancer Lett.*, 2007, **248**, 321–331.